**Determining background signatures and finding unusual objects in multi-dimensional data cubes**

STANLEY R. ROTMAN[A], JERRY SILVERMAN[B] AND CHARLENE E. CAEFER[C*]

[A]Ben-Gurion University of the Negev, Department of Electrical and Computer Engineering,

P.O. Box 653, Beer-Sheva, Israel

[B] Solid State Scientific Corp., 27-2 Wright Rd., Hollis NH 03049

[C]Air Force Research Laboratory, AFRL/SNHI, 80 Scott Road, Hanscom Air Force Base, MA 01731, USA

[*]Corresponding author. Tel.: +1-781-377-2875; fax: +1-781-377-4814.
E-mail address: charlene.caefer@hanscom.af.mil

**Abstract.** We describe and demonstrate a method to detect unusual objects in segmented visible or infrared multi-dimensional imagery with minimum operator intervention. One assumes that the largest segments characterize the background and uses these segments to generate a set of average profile signatures to represent this background. Several methods are then compared for finding and emphasizing pixel anomalies from this background. Finally, morphological operations are used to find unusual objects composed of such pixel anomalies. Initial experimental results on a set of four HYDICE hyperspectral data cubes indicate that the technique could serve as a powerful target-cueing step in many applications.

## 1. Introduction

When one obtains an image or a sequence of images of real scenes in either the time or spectral domain, the first step of the analysis is often to segment the image to allow for better computer vision or human analysis. The initial segmentation results allow for each resulting segment to be analyzed independently of the rest of the image. We have recently developed a simple and reliable technique for segmenting multi-dimensional data cubes (Silverman et al. 2002 a, b), which is histogram-based and avoids any spatial constraints. In the context of scene or material classification, the histogram-based approach and other approaches independent of spatial coordinates (Viovy 2000, Huang 2002) are often the most useful as unconnected regions may physically represent the same material and should be assigned the same segmentation level. More traditional edge-based techniques (Gonzalez and Woods 1993) or contiguous brightness methods (Duda and Hart 1973) are spatially dependent.

For the present objective, namely detecting unusual objects made up of anomalous pixels in multi-dimensional data cubes, we are not interested in all the segments in the image, but only in those which do not fit into the overall background of the image. To do this, prior knowledge of the natural background of the image would be desirable. Lacking this information, we need to define those segments which represent background in order to allow us to distinguish those pixels which do not fit. We assume that the largest areas of the image are characteristic of the natural background of the image. Several methods are then proposed to distinguish anomalous pixels which don't fit these background signatures. Groups of anomalous pixels that pass a morphological test in having the proper shape and size will then be considered as unusual objects of interest. While the examples in this paper will be data cubes whose successive layers are based on different spectral wavelengths, the method suggested will be appropriate for any multi-dimensional cube.

The organization of our paper is as follows: Sections 2.1 – 2.5 describe several approaches in going from segmentation to object identification including digital morphology, anomalous pixel detection followed by analog morphology seeking the unusual object, and segmentation as a feed-in to a standard sub-space projection algorithm; Section 3 presents discussion, conclusions and future directions.

## 2. Techniques for detecting unusual objects

### 2.1. *Background determination*

We assume that we have available to us a segmentation of the data cube which has successfully grouped pixels into clusters having similar signatures. Our first goal is to use this segmentation to determine the background signatures of these natural scenes.

For this purpose and in order to avoid anecdotal examples and quantify our results, we use a set of four HYDICE spectral data cubes, scenes 1 to 4, of roughly the same ground area. The data was taken over the ARM site (HYDICE 1997) over three days in June, 1997 at 4:30, 5:30, 5:37, and 12:20 PM respectively. Scenes 1, 2 and 4 were taken at about 6000 ft. and scene 3 at 5000 ft. The scene content consists of plowed farmland, a road, a triangular shaped region of trees, and three panels (assumed for the present application to be the *unusual objects* not fitting into the overall background).

**Insert figures 1 and 2**

Figure. 1 shows sample frames from each scene; figure 2 shows segmentations of the four scenes to 6, 5, 8 and 5 levels respectively (Silverman and Rotman 2003). Note that many of the panels segment almost completely to one digital level but some, like the upper panel in fig. 2b or the panels in fig. 2c, are hybrids of two digital levels. This has significant consequences for the approaches to be discussed. Figure 3a shows representative profiles of a ground, road and panel pixel, while figure 3b shows a pair of profiles from each of the three panels. The closely matching pairs are from the same panel and indicate that the main distinction between panels is a scaling constant, which is true for all four scenes.

**Insert figure 3**

2.2. *Morphological preliminaries*

Since all our approaches entail morphological post-processing, we briefly review some basic morphological operations (Rivest and Fontin 1996). Consider the following sequential operations. After specifying a rectangular region, x pixels by y pixels, one applies an erosion (minima) followed by a dilation (maxima) of size x by y at each pixel oriented appropriately with respect to the region. If one applies the operations directly to the image, positive contrast features x by y pixels (or larger in each dimension) are retained, so-called morphological "openings". By subtracting the result of openings from the original image, one retains features of positive contrast smaller than x pixels in the first dimension or smaller than y pixels in the second, so-called "white hat" operations.

While we have explored combinations of openings and white hats in either rectangular form (as just described) or generalized to diagonal oriented features, we take a still more general approach by assuming in the following sections that only the minimum and maximum dimensions of the unusual objects of interest on the focal plane are known with no available information on orientation. After defining square regions of interest, we will apply our morphological operations in the manner indicated in the next section.

2.3. *Direct application of morphology to digital segmentations*

For clarity, we will reserve the term *segment* to refer to all the pixels in a segmented image with the same digital value. For example, in scene 4 (figure 2d), the white segment (digital value 5), forms the bulk of the lowest panel but many road pixels have the same segmentation value. We reserve the term *segmented region* for a spatially contiguous region, such as the upper panel in scene 4, segmented to the same value, regardless if there are other pixels elsewhere assigned this same value. The simplest approach is to apply binary morphological operations

independently to each digital level, i.e. form a separate black/white image from each digital level, and attempt to extract desired *segmented regions.* For the panels in these scenes, we choose 4 and 16 pixels for the extreme dimensions and apply the following rectangular morphological operations: a 4 by 4 opening and a pair of 1 by 16 and 16 by 1 white hats. By logical anding of these operations, we retain *segmented regions* within a minimum window size of 4 by 4 pixels and a maximum window of 15 by 15 pixels.

The results of the above operations applied to the segmentations of figure 2 are shown in figure 4 and illustrate the problems with this approach. If the panels exist as *segmented regions* as in figure 2a and 2d, one recovers them almost in toto (figure 4a and 4d). If however the panels exist as hybrid segmentations, one can lose a whole panel (figure 4b) or recover just fragments (4c). An additional drawback of this approach is the lack of magnitude differentiation among the recovered *segmented regions.* Further operator intervention such as crosschecking back to the original data cube would be needed to weed out the false alarms. The approach outlined in the next section, which postpones the morphological steps until after an anomalous pixel (analogue) detection stage, ameliorates these problems.

**Insert figure 4**

2.4. *Use of analogue detection images and analogue morphology*

As shown in the last section, the direct use of the segmented image to detect specific unusual objects requires a proper segmentation of the object from the background. When the object is composed of different types of materials or temperature zones, more complicated segmentations may result. Further, parts of the object may be included into background segments. In either case, morphological reductions directly from the segmented images become problematical.

To circumvent these problems, we have developed an analogue detection stage to follow the segmentation and to precede the morphological operations. We start with the following basic assumptions:

1. The desired unusual objects occupy a small fraction of the total image.

2. The average signatures of background segments accurately represent the signatures of the background pixels and are distinct from the unusual object signatures.

Our analogue detection process is set up as follows. The *segmented regions* are ranked in order of size. We assume that a fraction X of the pixels constitutes background: X is typically chosen in the range from 0.90 to 0.98. Starting with the largest *segmented region*, we add the *segmented regions* in turn until we have reached the specified X.

When this is done we have a number of segments which are assumed to constitute background (including all the remaining pixels with the same digital values as the chosen *segmented regions* so that the final fraction is typically $\geq$ X); the remaining segments are defined as candidates to contain the unusual objects sought. We form a representative signature for each background segment by averaging over all the pixel signatures in that segment from the original datacube. Hence we have reduced our background to a set of average vectors derived from the largest segmented units.

**Insert figure 5**

In figure 5, we use the scene 1 segmentation (figure 5a) to demonstrate this *background cueing* process. Digital segments labeled 1, 2, and 4 (ground, plowed areas, and road sections respectively) form three background segments and constitute 93% of the image. The 7% remaining pixels are candidate unusual object pixels (deep blue regions in figure 5b). To generate our anomalous pixel analogue detection output, each pixel in the image is compared to each average background signature. Two metrics are tested: the Euclidean distance and the spectral angle measure (SAM) between the pixel signature and the average signatures (Schowengerdt 1997). For each metric, the value assigned to the pixel is the minimum value of the metric obtained with respect to any of the background signatures. Hence, pixels with higher values have poorer matches with all the background signatures. The pair of images obtained in this fashion (Euclidean and angular measures) are shown in linear display in figures 5c and 5d.

We complete the processing by applying the same morphological operations used above to these gray-scale analogue detection images. (Note that in the digital domain, each digital level is treated as a distinct black/white image in the morphological processing; while in the gray-scale domain, the morphological operations are applied to a single analog image. Hence, adjacent regions might interfere and modulate each other in the analog mode.) The morphological outputs (figures 5e and 5f) extract the panels as well above almost all the remaining pixels.

We show the corresponding processing sequence for scene 4, the most challenging of the scenes, in figure 6. For this case, digital segments 1 and 2 of ground pixels constitute 96.4% of the image as background and segments 3,4, and 5 (deep blue in 6b) are the candidate unusual object pixels. Since the panels pixels here are closer in magnitude to the background than isolated bright pixels in the scene, the Euclidean measure gives poor results (figures 6c and 6e), but the angular measure still produces excellent results (6d and 6f).

**Insert figure 6**

In figure 7, we show angular measure results for scenes 2 and 3 which are of comparable quality to those for scenes 1 and 4. For scene 3 (figures 7c and d), the outer morphological dimension is increased to 18 pixels to accommodate the larger finger print; some gray-scale variations are apparent in the morphological output of this scene.

**Insert figure 7**

In the absence of ground truth, we used the following simple procedure in generating ROC curves for the above results. From the segmentation of each scene, we tally the total number of pixels on the three panels, giving the total number of unusual object pixels, $N_T$, (only in scene 2, where border panel pixels differ both from the background and the full panel pixels, is this number not clear cut). For each analogue detection image at a given threshold, we determine a point on the ROC curve as: $P_D = N_{PANEL} / N_T$ and $P_{FA} = N_{NON\text{-}PANEL} / N_{SCENE}$, where the numerators are the number of panel and non-panel pixels above threshold and $N_{SCENE}$ are the total number of pixels in the scene.

ROC curves for scenes 1 and 4 are shown in figure 8. Generally there are 4 ROC curves for each scene: namely, the curves for the analogue detection image itself and the morphological output from the analogue images for each of the measures, Euclidean and angular. For this limited data set, the angular metric is the more reliable. (We omit the poor ROC curve for the Euclidean measure in scene 4 before morphology.) For all scenes, after application of the morphological operations on the analogue detection images based on the angular measure, 80 % or greater of the panel pixels are detected with none or few non-panel pixels, i.e. false alarms.

**Insert figure 8**

2.5. *Automated orthogonal subspace projection.*

Techniques pioneered by Chang and Ren (Chang and Ren 2000) use a set of background signatures to define a subspace in the data cube and then project the signature of a test pixel orthogonal to this subspace. In the original and most basic version of these subspace algorithms (Harsanyi 1993), the Orthogonal Subspace Projection (OSP), one completes the algorithm by taking a dot product (matched filter) between a known object signature and the orthogonal component of the test pixel.

$$OSP = p_i \mathbf{P} d^T \quad (1)$$

where for an image of n bands, $p_i$ is the 1 by n vector of the test pixel signature, $d$ is the 1 by n target signature vector and $\mathbf{P}$ is an n by n projection matrix.

$$\mathbf{P} = \mathbf{I} - \mathbf{U}\mathbf{U}^{\#} \quad (2)$$

where $\mathbf{U}$ is n by k matrix whose k cols are signatures defining the k background components and $\mathbf{U}^{\#} = \left(\mathbf{U}^T\mathbf{U}\right)^{-1}\mathbf{U}^T$ is a pseudo inverse of $\mathbf{U}$. We use a simple and automated form of the OSP to generate alternative analogue detection images to those used in the last section. The $\mathbf{U}$ matrix is formed from the average background signatures generated by the above *background cueing* process from the segmentations and then each pixel in turn is used as the target signature $d$ in a non-target form of the OSP (NTOSP):

$$NTOSP = p_i\mathbf{P}p_i^T \quad (3).$$

The NTOSP generated analogue detection images are post-processed by the same morphological operations as the previous section. Generally the corresponding ROC curves are quite similar to the set in figure 8 with some examples shown in figure 9 where we compare the angular metric results on scene 1 and 4 taken from figure 8 with the ROC curves for the NTOSP.

2.6. *Final comments on techniques*

The approach of generating an analogue detection image cued by the segmented image appears to be a very powerful and robust technique for detecting unusual objects. Consider the following alternative occurrences at the background-cueing stage of this technique. 1. The desired unusual object (e.g. the panel) is part of the (100-X)% of the non-background pixels and represents a *segmented region* in the original segmentation. 2. The desired object is also part of the (100-X)% of the pixels but is not a *segmented region* in the original segmentation but is a hybrid of non-background levels. 3. Portions of the desired object are segmented with the same levels as background segments. 4. The desired object was one of the chosen *segmented regions* taken as constituting background. (Note that we try to avoid this last possibility by not allowing X to approach too closely to 100%.)

Of the four cases described, the first is clearly optimal. In that case, the object should be detectable by the segmenting and morphological procedures described in Sections 2.3 or 2.4. The other three cases are likely to fail for the direct digital morphological method (2.3), while cases 2 and 3 are still quite viable for the analogue morphological approach (2.4). For case 2, the object pixels have not influenced the background average pixel signatures and one would detect these pixels as being distinct from the background. As for case 3, if the background pixel levels are much greater in number than the object pixels similarly labeled, then the particular features of the object pixels that distinguish them from the background may not enter the average background signature and our analogue detection method will still work. Only in the fourth case, where the object entered the background as its own *segmented region* does one expect difficulty in detecting the object.

The OSP method (2.5) theoretically has certain potential benefits over the analogue morphological detection method of subsection 2.4. By projecting out of the subspace defined by the background vectors, we should potentially have fewer errors with mixed pixels found at the edges between two background segments. The analogue detection method should find these pixels as anomalous (and hence potential false alarms), since the comparison to the background signatures is done sequentially rather than in a matrix formulation (as in the OSP). It is therefore surprising and interesting that the analogue detection approach performs almost as well as the OSP method (especially after the morphological stage) since the former, not involving matrix inversions, is computationally simpler than the OSP approach.

We offer several conjectures to explain the above. First, morphological operations upon the analogue detection images stages eliminate many of the potential errors; thus, the simpler method is adequate to generate the desired unusual objects even if more false anomaly pixels are present in the analogue detection stages. One notes for example in figure 9a that the better performance of the NTOSP before morphology is largely removed after morphology. In addition, due to the relatively small number of edge pixels in the image, weaknesses in the performance on the edge pixels would not be as noticeable. In scene 2 (not shown), border pixels on the edges of the panels are stronger relative to hybrid pixels in the background in the NTOSP method than in the simpler analogue detection method, a difference that persists to some extent after morphology. Finally, the NTOSP method removes from each vector the components that are in the subspace of the background endmembers; this will occur even if the background endmember is infrequently found in the image. This could be deleterious leaving very small

components of the desired object signature remaining. Further research is needed to analyze the effect of different number of background endmembers on the system performance.

## 3. Discussion and conclusions

A recent paper (Stein et.al 2002) divides anomaly detection algorithms into three classes and it is of interest to fit the present work into this taxonomy. Class 1 are algorithms based on differences between a central pixel and it's surrounding pixels ("Local Normal Model"); class 2 are algorithms which assign pixels to one of several groups, each group characterized by a Gaussian distribution, with the anomalies not fitting well into any group ("Gaussian Mixture Model"); class 3 are algorithms which try to fit each pixel to linear combinations of known or measured endmembers with anomalies those pixels having poor fit. Our techniques are closest to class 2, the Gaussian Mixture Model, with the important innovations that classes need not be Gaussian, flexible measures of fit can be used, and powerful morphological operations can select the pixel anomalies of interest.

Our methods of background characterization have some similarities to the Low Probability of Detection (LPD) method ( Harsanyi et al. 1994). For the LPD method, the subspace of the background signatures is assumed to be identical to that of the significant eigenvectors from the PC analysis. With the assumption that the objects are very small and, hence, the object signatures do not affect the leading eigenvectors, an estimate of the background subspace is made. The LPD method does assume that the object signature is known; a matched filter is applied after one projects the suspect pixels into the space orthogonal to the background subspace.

In the algorithms of sections 2.4 and 2.5, we make an assumption similar to the LPD algorithm, i.e. that the desired unusual object(s) is(are) a small fraction of the background. We derive the background signatures not through the use of the principal eigenvectors, but by using the average signatures of the largest segments produced by the segmentation algorithm. The object signatures are not known; the potential non-background objects are found by their difference from the background signatures, as measured by either Euclidean distance or angular distance (SAM). In addition, we tried projecting all suspect pixels into the subspace orthogonal to the background pixels. An analog morphological methodology was then used to post-process the candidate pixels to find those of the proper size and shape. Whether one uses the OSP or the simpler analogue detection technique of section 2.4, such image processing algorithms offer a promising method for using segmentations to generate background

signatures. These background signatures can then be used to generate analogue detection images followed by the application of analogue morphological operations.

We have already demonstrated that our segmentation techniques work in several bands (Silverman et al. 2002 a, b). The excellent initial results on Hydice images suggest that the sequence of segmentation/analogue detection image/morphology should prove effective as well on other data sets in finding unusual objects (Silverman and Rotman 2003). We look forward to applying these methods on data from other spectral bands as well as on data sets created in the time domain. The methods have great potential as a powerful target-cueing step in many applications.

**Acknowledgements**

The HYDICE data was provided by the Spectral Information Technology Application Center (SITAC). This work was carried out under Air Force Task 2305BN00. We'd like to acknowledge partial support of the Paul Ivanier Center for Robotics and Industrial Production, Beer-Sheva, Israel. This work was performed while one of the authors (SRR) held a National Research Council Research Associateship Award at the Air Force Research Laboratory at Hanscom AFB.

**Figure Captions**

Figure 1. A sample band image for each of four HYDICE scenes used to test the present techniques; scenes 1 to 4 are from left to right, top to bottom respectively.

Figure 2. Corresponding segmentations of the four scenes to 6, 5, 8 and 5 levels respectively.

Figure 3. Typical signatures from the four scenes: (left) a ground, road and panel pixel; (right) a pair of pixels from each of the three panels.

Figure 4. Corresponding digital morphological outputs of the segmentations of figure 2. See text for details.

Figure 5. Processing sequence applied to scene 1. (a) Segmentation as in figure 2. (b) Background cueing result with non-background pixels (candidate anomalies) in deep blue. (c) and (d) Analogue detection images based on Euclidian and Angular metrics respectively. (e) and (f) Morphological outputs of (c) and (d). See text for fuller details.

Figure 6. Corresponding processing chain of figure 5 applied to scene 4.

Figure 7. Results from scenes 2 and 3. (a) and (c) Analogue detection images of scenes 2 and 3 respectively based on the Angular metric. (b) and (d) Morphological outputs from (a) and (c).

Figure 8. ROC curves for processing results on scene 1 (left) and scene 4 (right). Curves are keyed by an E or A to indicate Euclidean or angular measures, a following M indicates the morphological outputs.

Figure 9. Some ROC curve comparisons between the NTSOP (Non Target the Orthogonal Subspace Projection ) and the results of Figure 8 for scene 1 (left) and scene 4 (right). Curve notations as in Figure 8.

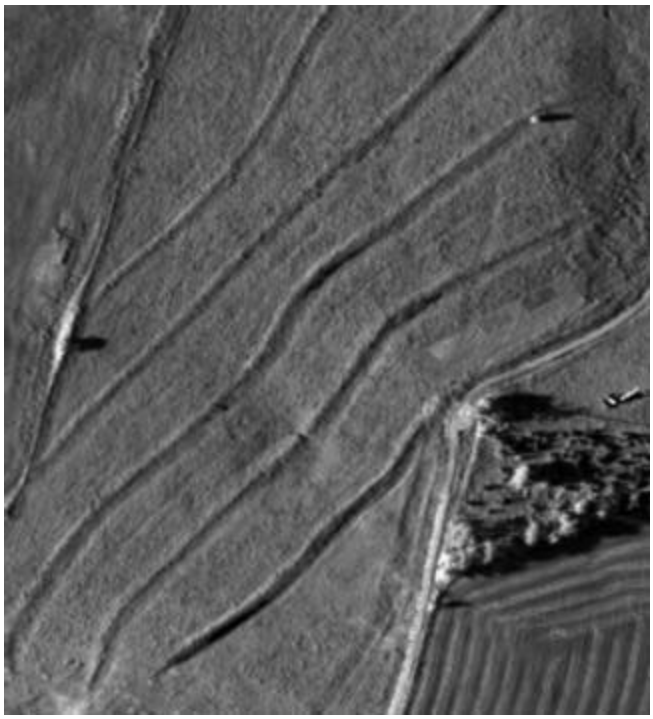

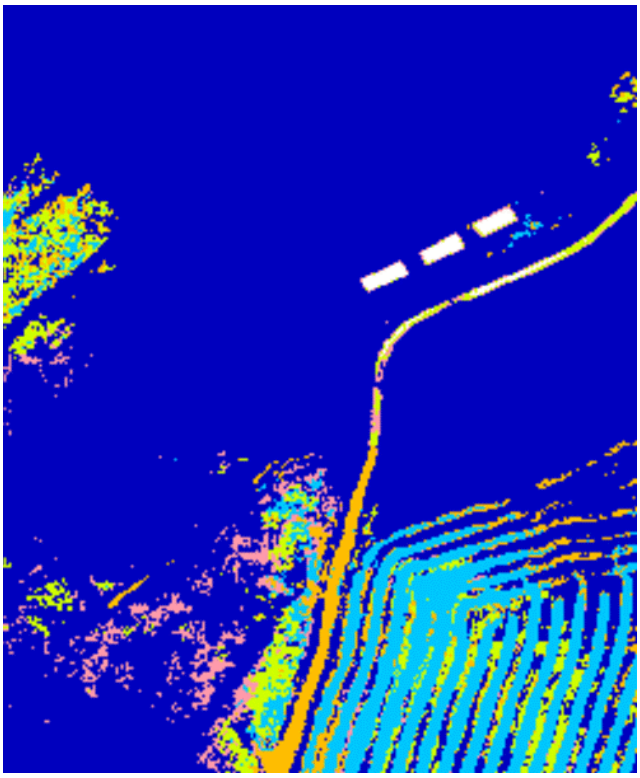

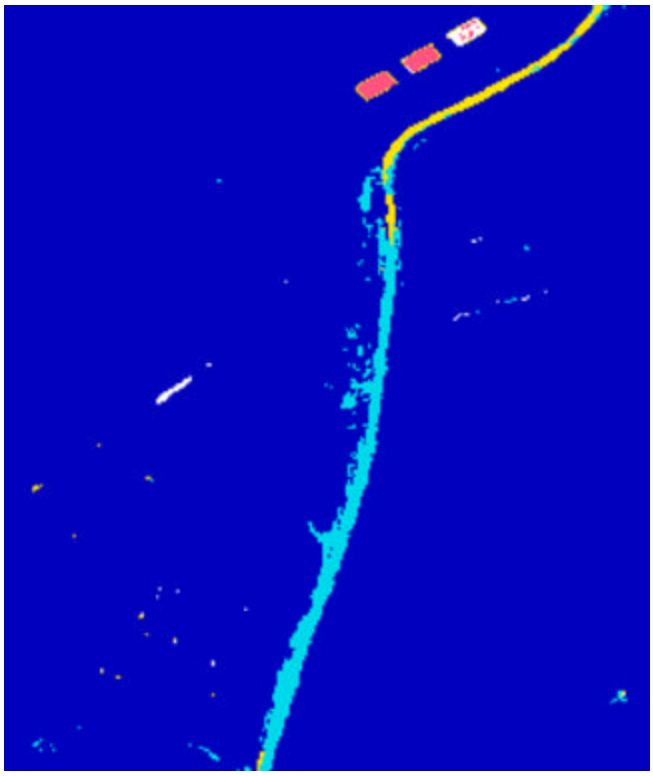

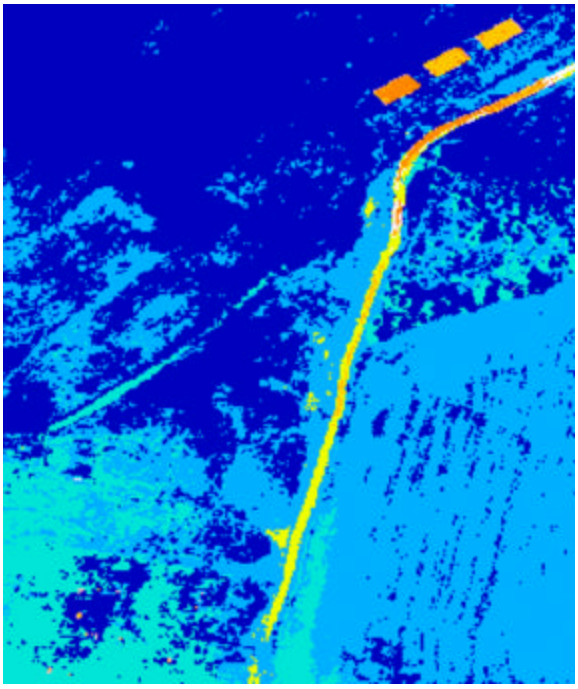

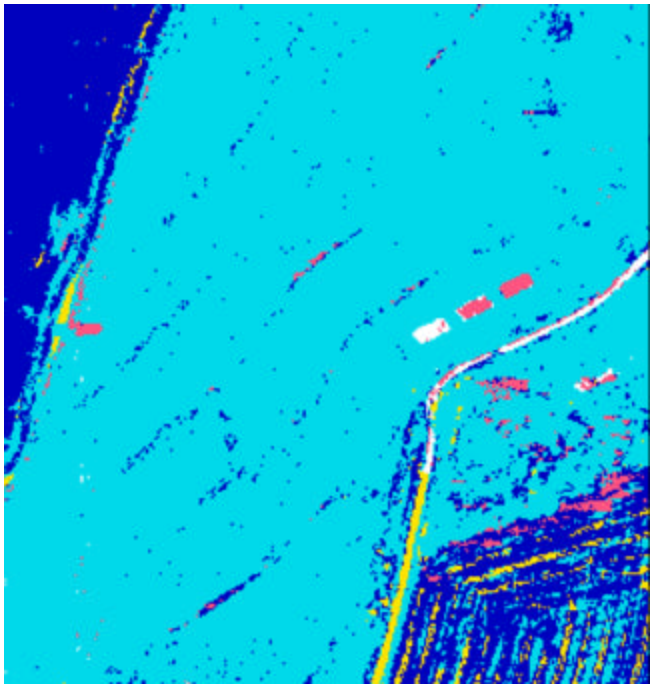

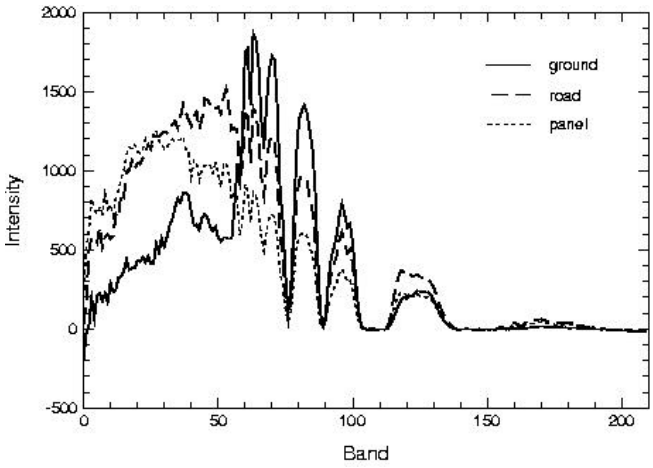
ground
road
panel
Intensity
Band
2000
1500
1000
500
0
-500
0
50
100
150
200

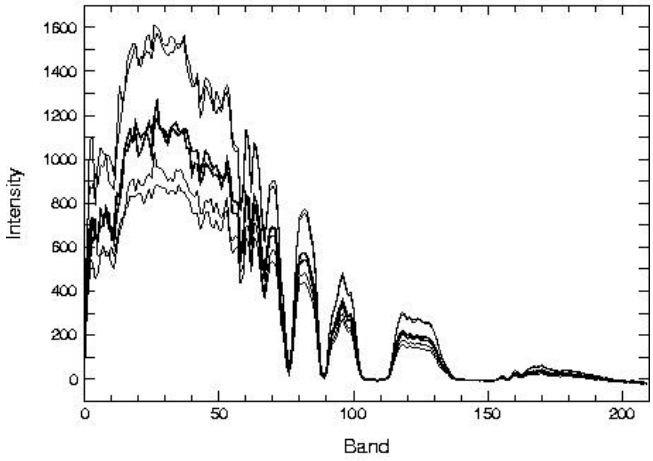
Intensity
Band
1600
1400
1200
1000
800
600
400
200
0
0
50
100
150
200

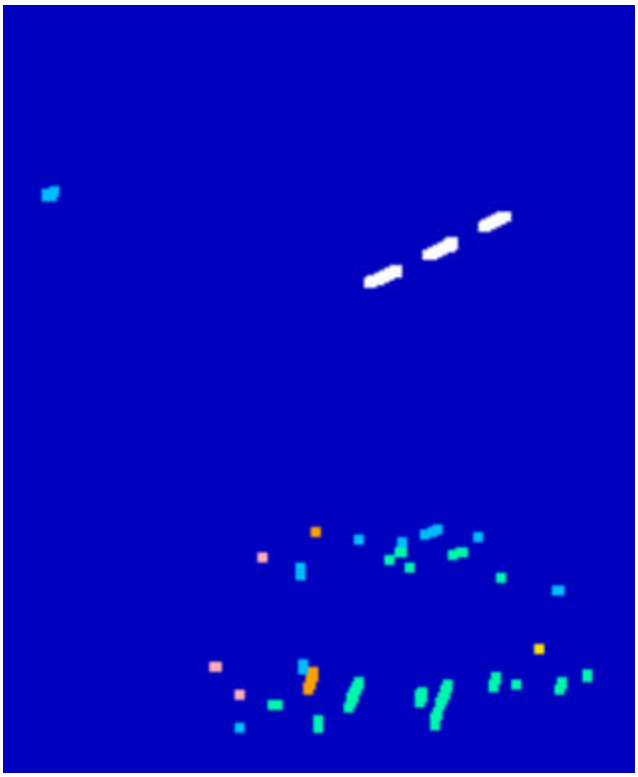

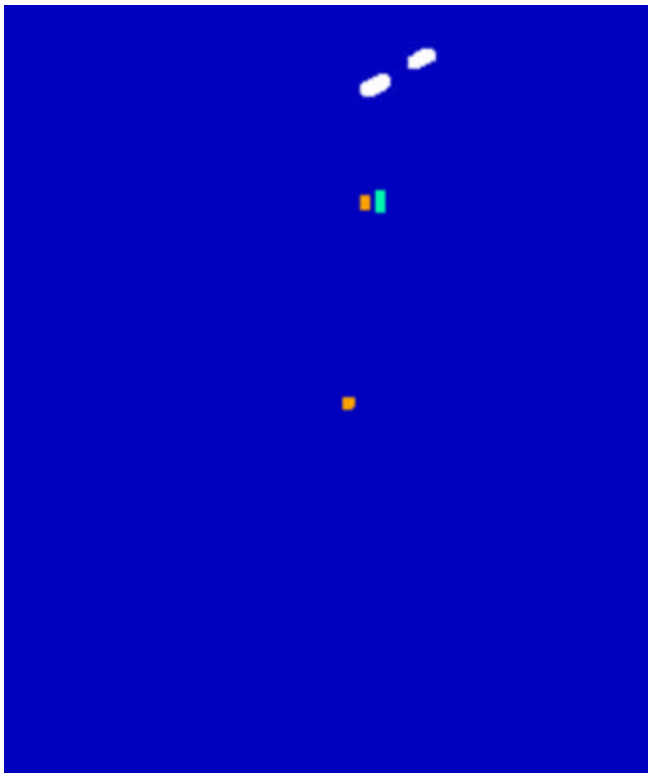

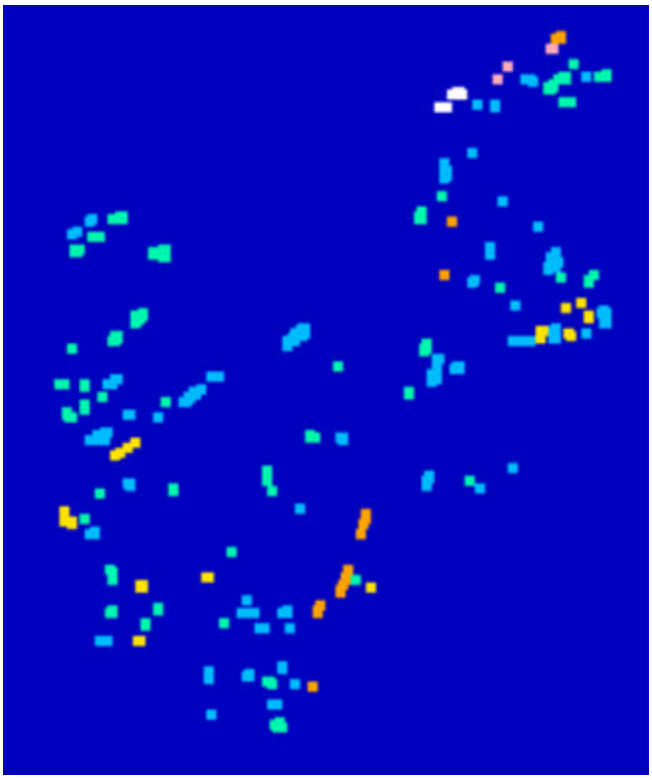

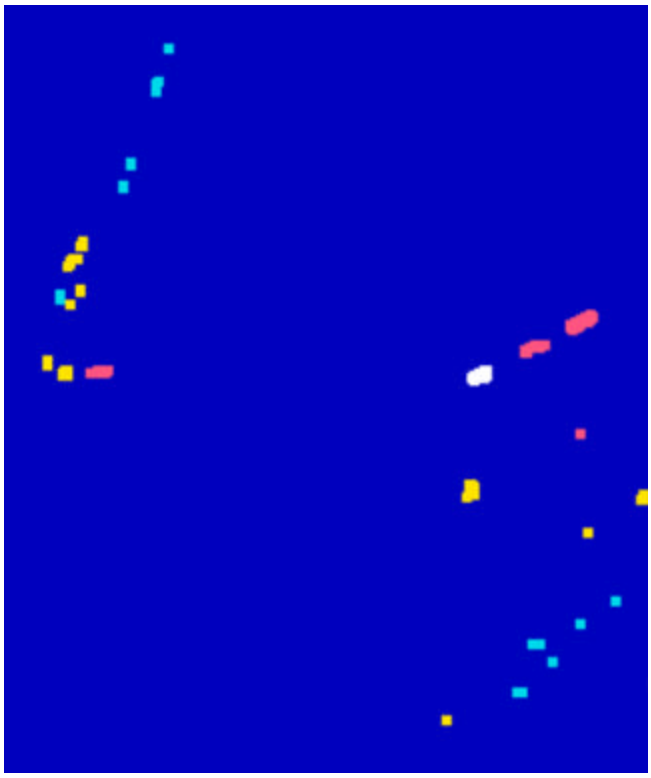

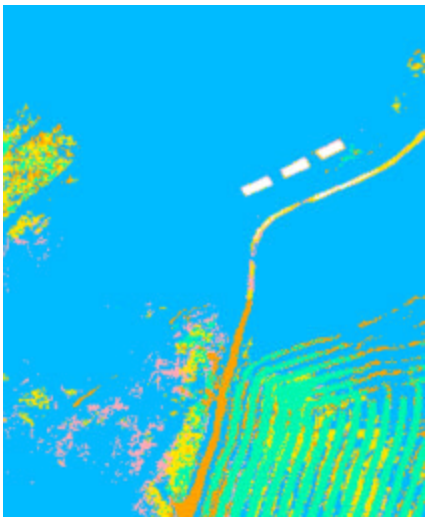

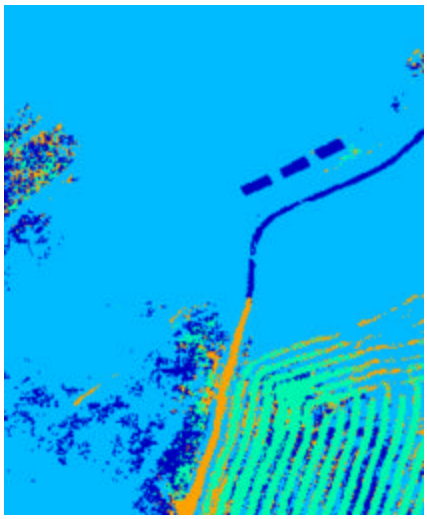

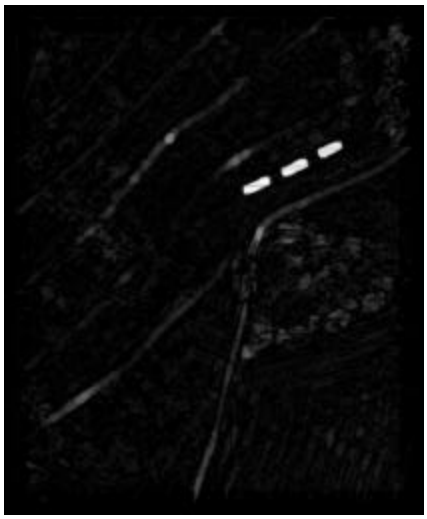

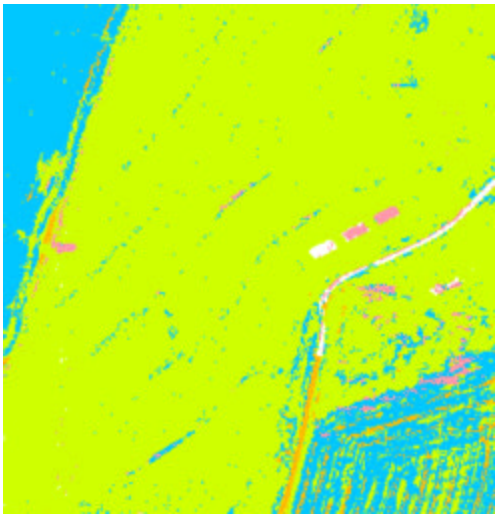

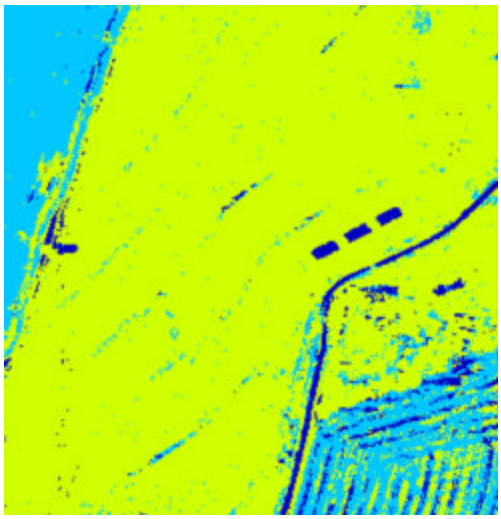

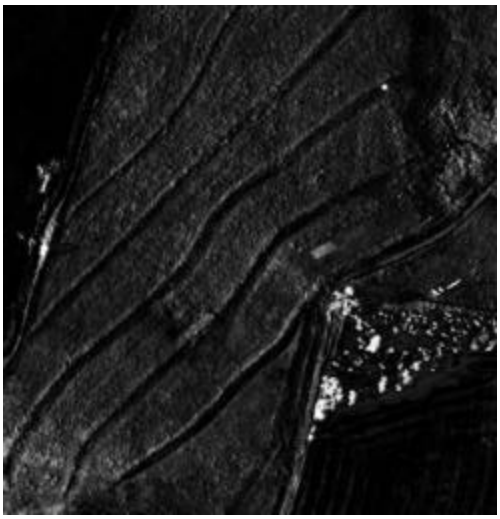

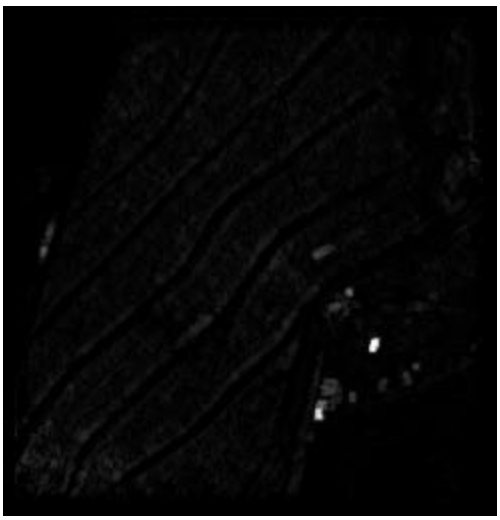

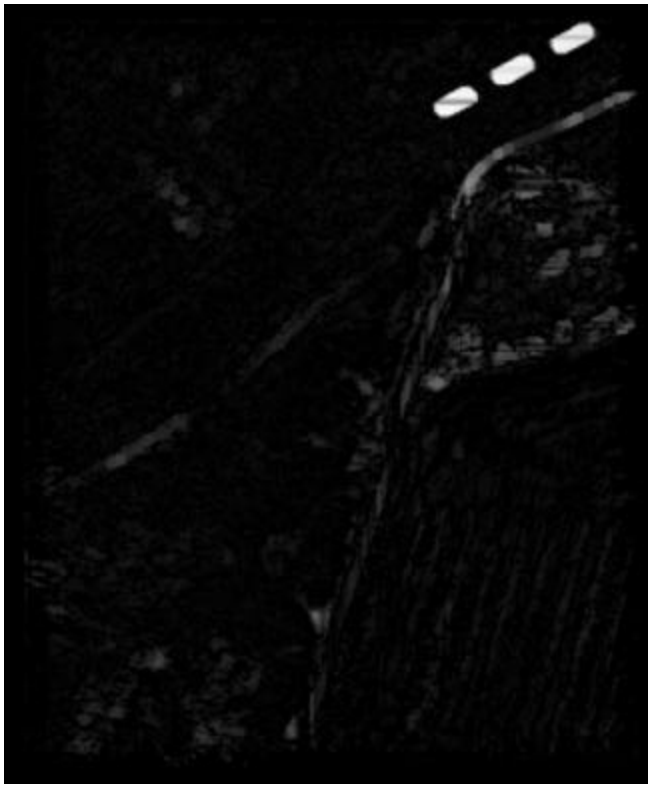

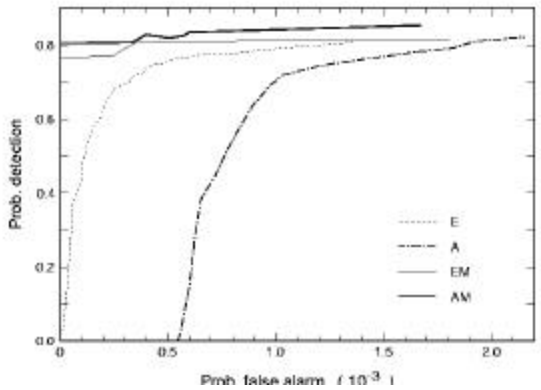
Prob. detection
E
A
EM
AM

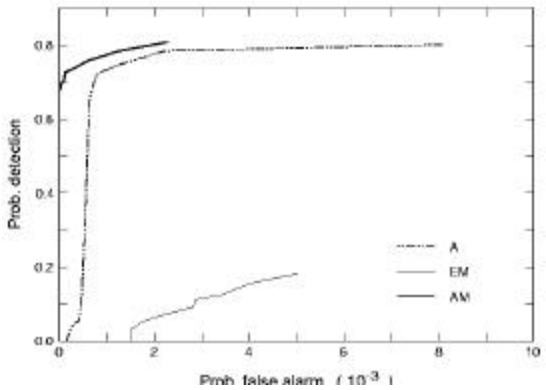
Prob. detection
A
EM
AM

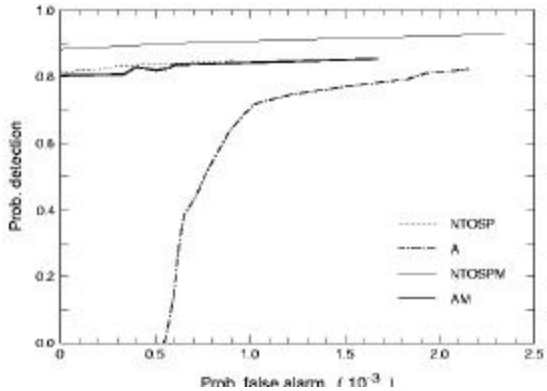
Prob. detection
NTOSP
A
NTOSPM
AM

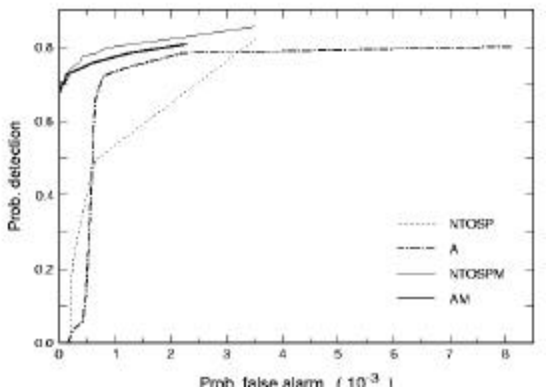
Prob. detection
NTOSP
A
NTOSPM
AM

**References**

CHANG, C.-I. and H. REN, 2000, An Experiment-Based Quantitative and Comparative Analysis of Target Detection and Image Classification Algorithms for Hyperspectral Imagery. IEEE Trans. Geo. Remote Sens. 38(2), 1044-1063.

DUDA, R.O. and HART, P.E., 1973, Pattern Classification and Scene Analysis, (New York: Wiley).

GONZALEZ, R.C. and WOODS, R.E., 1993, Digital Image Processing, (Reading, MA: Addison Wesley).

HARSANYI, J.C., "Detection and Classification of Subpixel Spectral Signatures in Hyperspectral Image Sequences", Phd Thesis, Univ. of Maryland Baltimore County, 1993.

HARSANYI, J.C., FARRAND, W.H., and CHANG C., 1994, Detection of Subpixel Signatures in Hyperspectral Image Sequences. ASPRS '94, pp. 1-15.

HUANG, K., 2002, The use of a newly developed algorithm of divisive hierarchical clustering for remote sensing image analysis. Int. J. Remote Sensing, 23, 3149-3168.

The HYDICE imagery, taken over the CART/ARM Site Lamont, was provided by the Spectral Information Technolgy Application Center (SITAC). HYDICE is a pushbroom imaging spectrometer with 210 spectral bands over the 0.4 to 2.5 micron spectral range.

RIVEST, J.-F. and R. FONTIN, 1996, Detection of dim targets in digital infrared imagery by morphological image processing. Opt. Eng. 35(7), pp. 1886-1893.

SCHOWENGERDT, R.A., 1997, Remote Sensing, (Boston: Academic Press), pp. 389-473.

a. SILVERMAN, J., CAEFER, C.E., MOONEY J.M., WEEKS M.M., and YIP P., 2002, An automated clustering/segmentation of hyperspectral images based on histogram thresholding. Imaging Spectrometry VII, Proceedings of SPIE Vol. 4480 pp. 65-75.

b. SILVERMAN, J., ROTMAN S.R., and C.E. CAEFER, 2002, Segmentation of hyperspectral images based on histograms of principal components. Imaging Spectrometry VIII, Proceedings of SPIE Vol. 4816 pp. 270-277.

SILVERMAN, J., ROTMAN S.R., 2003, Segmentations of hyperspectral imagery: techniques and applications. Infrared Technology and Applications XXVIII, Proceedings of SPIE Vol. 4820 pp. 334-349.

STEIN, D.W.J., BEAVEN, S.G., HOFF, L.E., WINTER, E.M., SCHAUM, A.P., and STOCKER, A.D., 2002, Anomaly detection from hyperspectral imagery. IEEE Signal Processing Magazine, January, pp. 58-69.

VIOVY, N., 2000, Automatic Classification of Time Series (ACTS): a new clustering method for remote sensing time series. Int. J. Remote Sensing, 21, pp. 1537-1560.